Surface Modifications of Expanded Poly(tetrafluoroethylene) Sheets Assisted by CO_2 Antenna Coupling Microwave Plasma

Y. W. Chen-Yang,*,† J. D. Liao,‡ J. Y. Kau,† J. Huang,§ W. T. Chang,⊥ and C. W. Chen†

Department of Chemistry, Chung Yuan Christian University, Chung-Li, Taiwan; Department of Biomedical Engineering, Chung Yuan Christian University, Chung-Li, Taiwan; Yeu Ming Tai Chemical Industrial Co., Ltd., Taiwan; and Department of Forensic Science, Central Police University, Taiwan

Received January 20, 1999; Revised Manuscript Received February 2, 2000

ABSTRACT: Surfaces of the expanded poly(tetrafluoroethylene) (ePTFE) sheets were chemically modified with the assistance of CO_2 cold plasma generated by antenna coupling guided microwave. The plasma pretreated ePTFE surface did not obviously change in terms of morphology of nodes structure but increased surface tension and promoted subsequent capability to graft polymerization with acrylic acid (AAc). The modified ePTFE were then characterized using FTIR-ATR and X-ray photoelectron spectroscopy (XPS). Morphologies of ePTFE surfaces and the cross-sectioned side of AAc-grafted ePTFE were examined by SEM and FTIR microscopy. Experimental results indicated that AAc penetrated to a depth of ca. 60 μm and bonded on the surfaces of nodes and fibrils. Generation of COF species on the ePTFE surfaces by CO_2 plasma contributed to this initiation effect. Current data also supported that plasma generated by the CO_2 antenna-coupling microwave system could efficiently activate the exposed ePTFE surfaces of interior fibrils and nodes. The variations of IR vibrational modes, binding energies of functional groups, and surface tensions were correlated with the chemical modifications applied on the ePTFE sheet. The mechanical strength of the pAAc-grafted ePTFE sheet appeared to be enhanced.

Introduction

Poly(tetrafluoroethylene) (PTFE) provides unique properties, such as low friction coefficient, high electrical resistance, low surface energy, and good thermal and chemical stability. On the other hand, the expanded PTFE (ePTFE) in sheet form has been widely used for separator in tightly pressed and varied chemical environments, owing to its hydrophobic surface, elasticlike characteristic, and porous property. By controlling the expanded pore sizes, the ePTFE sheets have valuable applications for biomedical-related purposes, such as semipermeable matters, selective membranes, and artificial blood vessels.[1−3] Nevertheless, the hydrophobic characteristic, which causes weak bonding capability for initiating surface adhesion with desired materials, has restricted the fluoropolymers for certain applications. Modification of fluorine-containing polymers has thus received extensive attention in terms of creating new chemistries that allow surface functionalization.[2,4]

Meanwhile, the use of plasma-associated techniques for polymer surface modification has recently grown rapidly.[5−9] The cold plasma technique is used to activate only the outmost surface of a material, without affecting its dimensions in a clean process. One characteristic of the plasma-induced radiation to polymers is to create short-lived free radicals and allow the effective energy of ionized species to transfer to the polymer surface.[6,10,11] Previous studies have discussed the possible function of free radicals and ionized species in plasma for reacting with polymeric chains.[6,12,13] Several comparative studies using various gas plasma treatments and surface-sensitive analytical instruments have been evaluated by Ratner,[3] Kang,[7,8] Ikada,[8] and Tran Minh et al.[14,15] Among various plasma generation sources, the radio-frequency types (∼13.56 MHz) have been more commonly used. However, microwave types (∼2.45 GHz) have the advantage of short treatment time to obtain a high degree of activated sites on a solid polymer. Although some results on the microwave plasma treatment of PTFE have been published, few results have been reported for the porous ePTFE.[15,16]

The comparison of antenna coupling microwave plasma with bias plates as capacitor containing radio-frequency plasma has been reported elsewhere.[6,17] It revealed that, under a similar distribution of supplying power, they differ in plasma ionization density by more than 10 times. Consequently, from the perspective of physical chemistry, the former plasma source would be relatively efficient to modify the matrix of ePTFE. In this work, a modified antenna-coupling microwave plasma system, which is also capable of providing a large valid treating area and uniform and high density ionized plasma, was used to activate the surfaces of a selected ePTFE sheet. The plasma pretreated ePTFE sheet was further grafted with acrylic acid (AAc) to increase its hydrophilicity. Chemical changes and wettability of the ePTFE surface were examined. Also investigated herein were the bonding and the depth of the graft copolymerization in the ePTFE matrix, which possibly influence its mechanical and chemical properties, as well as application potentials. Furthermore, cross-sectioned morphologies of the grafted samples were also studied to elucidate the penetration effect of AAc monomer.

Experimental Section

Sample Preparation. The ePTFE sheets used were commercially available from YMT Co., Ltd. Taiwan, designated as YMT1126, with specific gravity of 2.1 g/cm^2, melting point

† Department of Chemistry, Chung Yuan Christian University.
‡ Department of Biomedical Engineering, Chung Yuan Christian University.
§ Yeu Ming Tai Chemical Industrial Co., Ltd.
⊥ Central Police University.

10.1021/ma990065q CCC: $19.00
Published on Web 07/06/2000

of ca. 380 °C, and average pore size of ca. 1.0 μm. The sample sheets were prepared by Soxhlet extraction with methanol for 6 h followed by drying under reduced pressure. Synthesis-grade anionic monomer, AAc, from Aldrich Chem. Co. was vaporized, carried out by N_2, and used for graft polymerization.

Plasma Pretreatment. The equipment for performing the plasma treatment included a microwave plasma generator with maximum power of 2 kW, extensible 12 × 12 arrayed antenna elements, and a separated dielectric discharge chamber. The operating parameters were CO_2 gas flow rate of 5−10 mL/min, working pressure of 0.2 Torr, and plasma generation power of 600 W. Before the process, the chamber was purged with CO_2 for 6 min to clean out atmospheric ingredients.

Graft Polymerization. The ePTFE sheets of 3 cm × 10 cm treated by CO_2 plasma for 60 s were immersed in an aqueous solution of AAc (20 wt %) and stirred constantly under N_2 atmosphere at 65−80 °C for 1−24 h. Following graft copolymerization, the modified ePTFE sheets were washed with deionized water using a Soxhlet apparatus to remove pAAc homopolymer residue. Thereafter, the samples were rinsed and soaked in a gently stirred water bath at 80 °C for overnight, before finally being dried at 45 °C under a vacuum.

Measurements. Static contact angles were evaluated in air at 24 ± 1 °C using the sessile drop method. For each sample, every contact angle calculated was an average of 10 measurements with a standard deviation below 1°.

The element functionalities and new chemical bonding were investigated by using X-ray photoelectron spectroscopy (XPS): Physical Electronics/ESCA PHI 1600: Mg Kα 1253.6 eV, type 10-360 spherical capacitor analyzer with multichannel detector and $\Delta E/E$ of 0.1−0.8%. The takeoff angle was fixed at 42.5°.

Surface morphologies were examined by using scanning electron microscopy (SEM, JEOL-JSM-6300). Meanwhile, modes of molecular vibrations were detected by using a Fourier transformed infrared spectrometer (FTIR, Jasco-7000), equipped with attenuated total reflection (ATR, Jasco-500/M). The IR information on the cross-sectioned samples was evaluated using FTIR microscopy (Jasco-200) to determine the penetration depth of pAAc. For this measurement, a microtome of Universal Microtome Cryostat DDM-P500 was used to prepare the cross-sectioned thin film. Finally, mechanical properties of the ePTFE sheets were measured according to ASTM D-638 using Q Test V (MTS Ltd.).

To examine the morphologies of the cross-sectioned ePTFE samples using SEM, the sheet-form specimen was frozen in liquid nitrogen first and then split. It was then mounted onto a sample holder and gold-coated before examined using SEM. For FTIR microscopy measurements, a polypropylene film was used to envelope a pAAc-grafted ePTFE sheet to avoid contamination. The sample was mounted on the end of a slit dowel and immersed in epoxy resin in a silicone rubber cup. After the epoxy hardened, the silicone rubber cup was stripped away, and the chip-in-epoxy sample was sliced along the cross section to obtain a 15 μm thick thin film with a microtome. This thin film was straightened and flattened by pressing it between two 0.3 mm thick KBr plates before the experiments.

Results and Discussion

Chemical Changes of the Modified ePTFE Surfaces. Chemical changes to the modified ePTFE surfaces were determined with FTIR and XPS measurements. The IR-active vibrational modes of the untreated ePTFE resembled those of PTFE in different forms reported elsewhere.[13,18,19] The characteristic absorption bands of CF_3 deformation were found at 620−640 cm^{-1}. The strong absorbance at 1150 cm^{-1} was assigned to CF_2 stretching, while the absorbance at ca. 1240 cm^{-1} was assigned to CF_3 stretching. These absorbances remained unchanged after the modification. Meanwhile, as Figure 1 shows, a small absorbance is observed at 1881 cm^{-1}, indicating a slight presence of COF in the original ePTFE sheet due to the expansion process

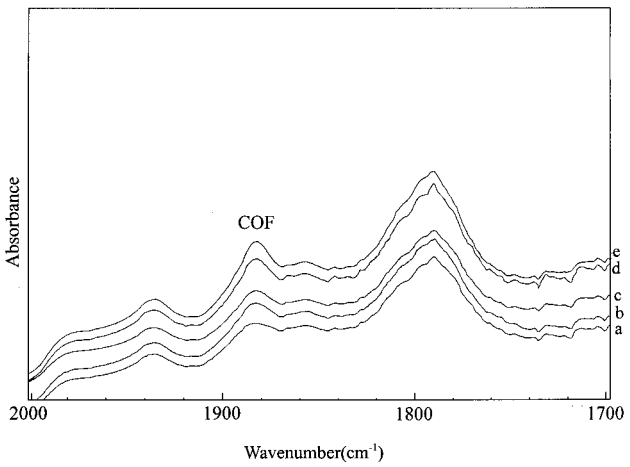

Figure 1. FTIR-ATR spectra of the ePTFE sheet with varied CO_2 microwave plasma treatment time: (a) untreated, (b) 1 min, (c) 3 min, (d) 10 min, and (e) 30 min.

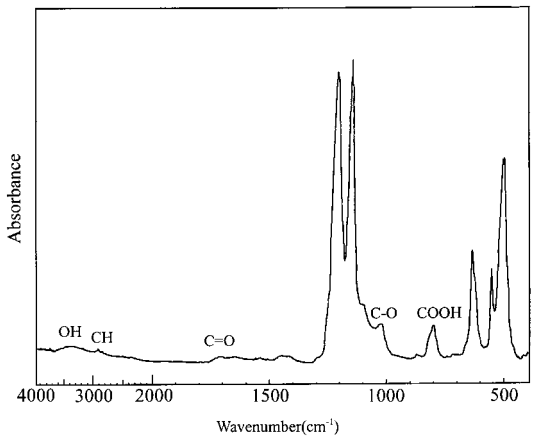

Figure 2. FTIR-ATR spectra of the pAAc-grafted ePTFE sheet with 60 s of CO_2 plasma pretreatment.

under high temperature. The absorbance is enlarged for the CO_2 plasma treated sample and slightly increases with treatment time. This increase is attributed to the production of COF species by the reaction of CO_2 plasma with the scissioned C−F bonds.

The graft polymerization of AAc with the plasma-pretreated ePTFE was confirmed by the main characteristic bands of pAAc at 3500 cm^{-1} (O−H stretching), 2980 cm^{-1} (C−H stretching), 1710 cm^{-1} (C═O stretching), 1020 cm^{-1} (C−O stretching), and 800 cm^{-1} (COOH out-of-plane deformation) as Figure 2 shows. The presence of these bands and the significant decrease of the 1881 cm^{-1} absorbance band implies that reactive or attractive forces existed between the AAc and COF species generated by the CO_2 plasma pretreatment. The attractive force may increase the penetration of AAc into the porous ePTFE matrix.

To monitor the graft polymerization of the pretreated ePTFE, the IR absorbance peaking at 800 cm^{-1} (COOH stretching) was compared with that at 638 cm^{-1} (C−F deformation) as described elsewhere.[20] As shown in Table 1, the ratio of the absorbance at 800 and 638 cm^{-1} increased with grafting time and reached a maximum at ca. 12 h, revealing that the amount of pAAc increased with grafting time and reached saturation at ca. 12 h. Meanwhile, the weight increase in the ePTFE sample was estimated by graft density using the gravimetric method, and this figure is listed in Table 1. A linear

Table 1. Graft Density, FTIR-ATR Absorbance Ratio, and XPS Atomic Ratio of the EPTFE Sheet with Respect to Grafting Time

graft time (h)	graft density (μg/cm^2)	A (800 cm^{-1})/ A (638 cm^{-1})[a]	XPS atomic ratio [F]/[C]	XPS atomic ratio [O]/[C]
0	0	0	2.14	0.022
1	1.2	0.46	1.43	0.083
2	4.5	0.54	1.23	0.117
3	10.6	0.67	1.21	0.142
4	6.8	0.72	1.07	0.140
6	20.3	0.76	1.09	0.129
12	24.6	0.85	1.03	0.123
24	26.8	0.86	0.98	0.124

[a] The ratio of the peak area at 800 and 638 cm^{-1}.

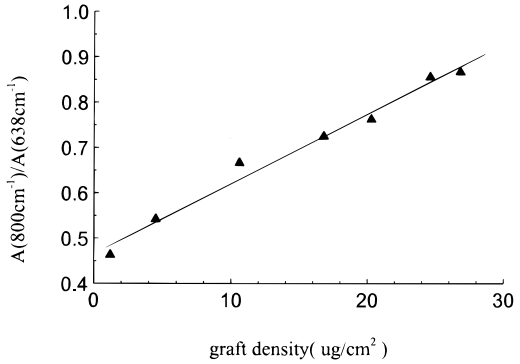

Figure 3. Relationship between the graft density measured by the gravimetry method and the IR absorbance ratio of the pAAc-grafted ePTFE sheet.

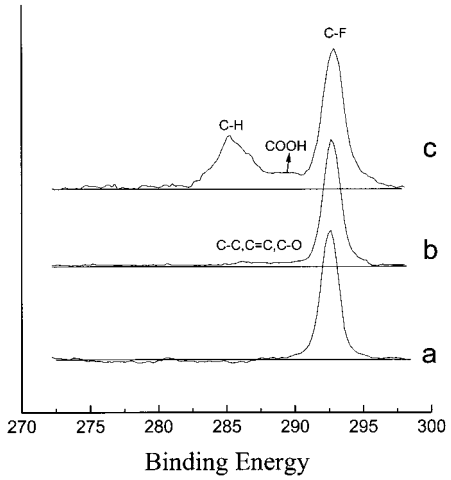

Figure 4. C 1s XPS spectra of (a) the untreated ePTFE sheet, (b) CO_2 plasma pretreated ePTFE sheet (60 s), and (c) the pAAc-grafted ePTFE sheet (1 h).

relationship between the absorbance ratio and graft density shown in Figure 3 reveals that the data obtained from the two methods agree well.

The elemental compositions of the ePTFE surfaces before and after modification were analyzed using XPS measurements. Figure 4a displays the C 1s core peak for the characteristic C−F bond of the untreated ePTFE at the binding energy of ca. 292.5 eV, which is taken as a reference. In Figure 4b, slight chemical shifts of the binding energies between 290.0 and 283.0 eV are observed for the CO_2 plasma treated sample, indicating that the treatment of CO_2 plasma involves oxygen-associate functions. This phenomenon resembles the result reported by Vasilets et al. for the PTFE film, in which the formation of COF-related species was suggested.[16] Meanwhile, for the pAAc grafted ePTFE sample, the strong peak of C 1s at 285.0 eV (Figure 4c) and the presence of O 1s at 532.0 eV (not shown) confirmed the grafting of pAAc. Furthermore, the peak intensity of F 1s at 689.5 eV decreased after plasma pretreatment and subsequent graft polymerization, as expected. As listed in Table 1, the F/C ratio dropped from 2.14 to 1.03 for the grafting time of 12 h, while the O/C ratio increased from 0.022 to 0.124, mainly because of the presence of pAAc. This finding corresponds to the result of previous IR measurements of pAAc on the ePTFE surfaces. Owing to the detection limit, the data were only meaningful for possible variation in the content of C, O, and F elements before and after the modification. Therefore, this result does not intend to interpret the depth of pAAc into the ePTFE matrix.

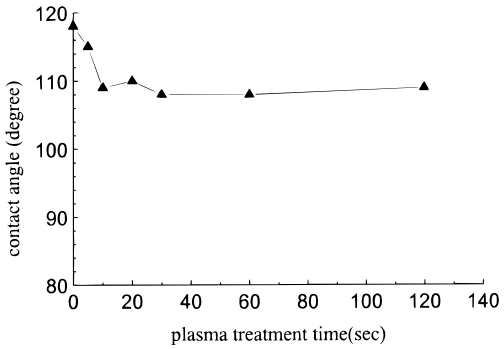

Figure 5. Plot of static contact angles of CO_2 plasma pretreated ePTFE sheet vs plasma treatment time.

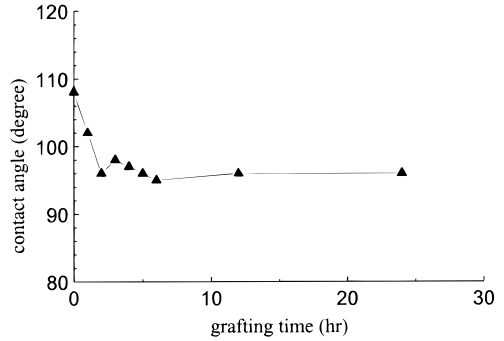

Figure 6. Static contact angles of the pAAc-grafted ePTFE vs grafting time.

Modification of ePTFE Matrix. To evaluate the degree of modification of the ePTFE matrix, static contact angle measurements, SEM, and FTIR microscopy were utilized. After CO_2 plasma treatment, the static contact angles of the ePTFE sheet decreased from ca. 118° to ca. 108° , as illustrated in Figure 5. The decrease was relatively large given such a short treatment time (60 s). This phenomenon may be attributed to the high ionization density of the plasma source used and the COF species generated. A further decrease of ca. 16° (from 108° to 92°) was obtained for the pAAc-grafted samples, as illustrated in Figure 6, and attributed to the hydrophilicity of the pAAc grafted on the surface of the sample.

Morphological change is generally a concern for pursuing surface modification. As Figure 7a displays, the SEM micrograph shows that the untreated ePTFE sheet is comprised of evenly distributed pores and nodes, interconnected three-dimensionally with the stretched fibrils formed during the biaxial expansion.[21] Figure

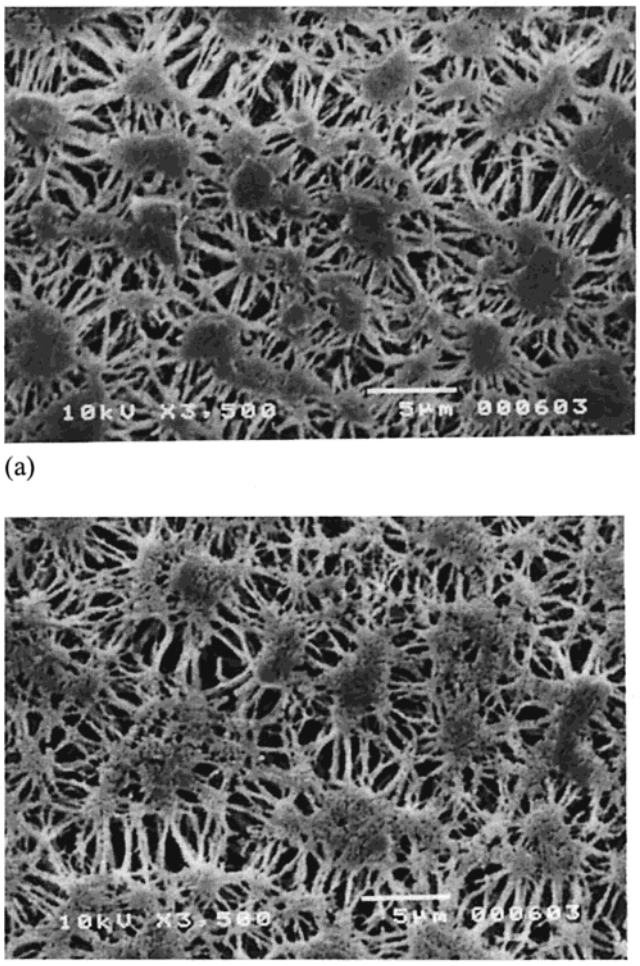

Figure 7. SEM micrographs of the ePTFE sheet: (a) untreated; (b) CO_2 plasma treated (60 s).

7b reveals no obvious change for the CO_2 plasma-modified ePTFE surfaces. However, the nodes began to be gradually dented by plasma treatment when exposure time exceeded 60 s. This phenomenon indicates that the surfaces of ePTFE were modified by CO_2 plasma, as exhibited by the decrease of static contact angles discussed above, but the morphology remained largely unaltered. With longer treatment, structural remolding, such as etching and cross-linking, became evident, and a thermal effect (for example, energy accumulation inside the matrix) could not be excluded.

Following graft polymerization with AAc, the morphology of the ePTFE sample differed from those of the untreated and the plasma treated samples. As Figure 8a shows, grafted pAAc was evenly deposited on the surfaces of the nodes and fibrils. This pattern implies that the CO_2 plasma used could distribute evenly on the surfaces of nodes and fibrils of the ePTFE sheet and hence activate the surfaces consistently. The degree of AAc polymerization increased with grafting time, as did the density (or accumulation effect) of the deposited pAAc and the amassing of the nodes and fibrils by the grafted pAAc, as shown in Figure 8b,c.

To further understand the penetration capability of the ionization plasma and AAc monomers beneath the surface of the ePTFE sheet, the samples were split under $N_{2(g)}$ to obtain a cross section of the ePTFE sheet. In Figure 9, the SEM micrographs show that after graft polymerization the nodes and fibrils by layers close to

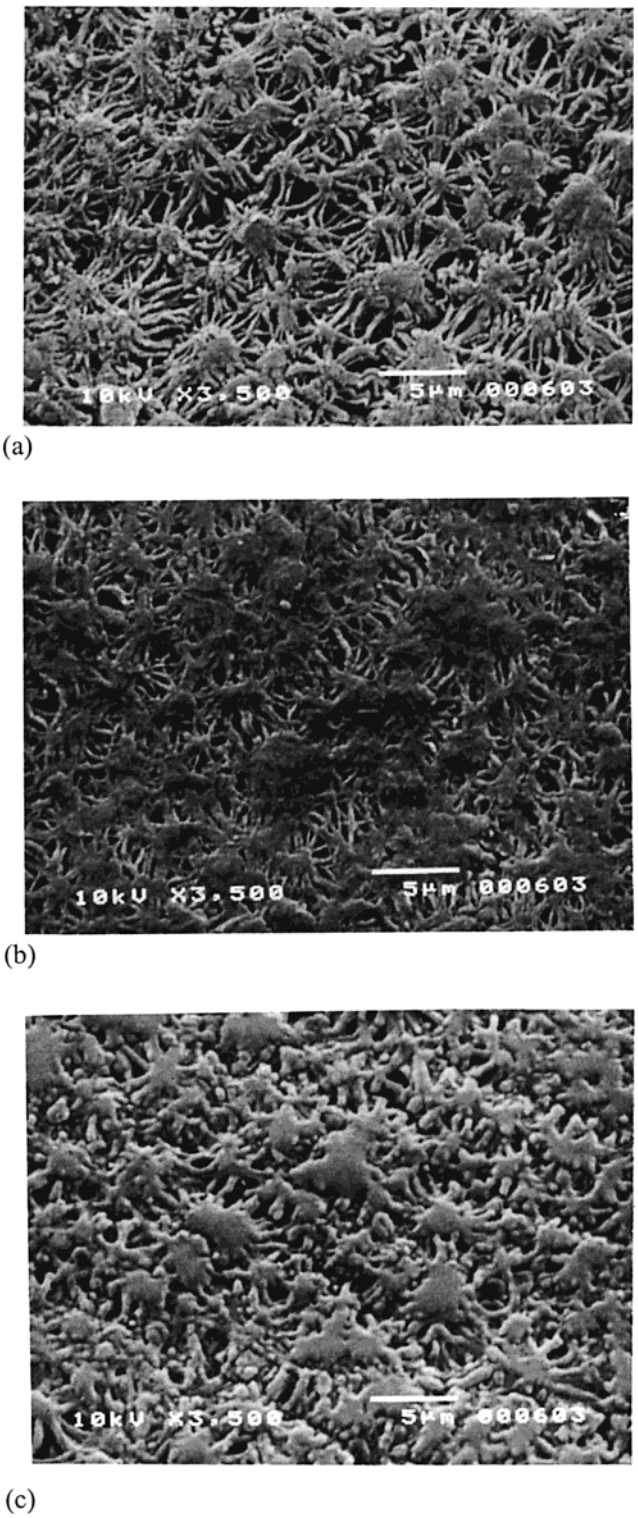

Figure 8. SEM micrograph of the pAAc-grafted ePTFE sheet with grafting time of (a) 1 h, (b) 2 h, and (c) 3 h.

the outmost surface are closely attached by the grafted pAAc, and the apparent density decreases gradually with sheet depth. This observation demonstrates that the inside surfaces of nodes and fibrils were also activated by the penetrated CO_2 plasma. With increasing depth, the migration of AAc monomers into the ePTFE matrix decreased because of the decrease of ionization density of the CO_2 plasma. SEM micrographs suggest a penetration depth of roughly ca. 60 μm.

To accurately measure the depth of pAAc penetration into the ePTFE matrix, the cross-sectioned surface of

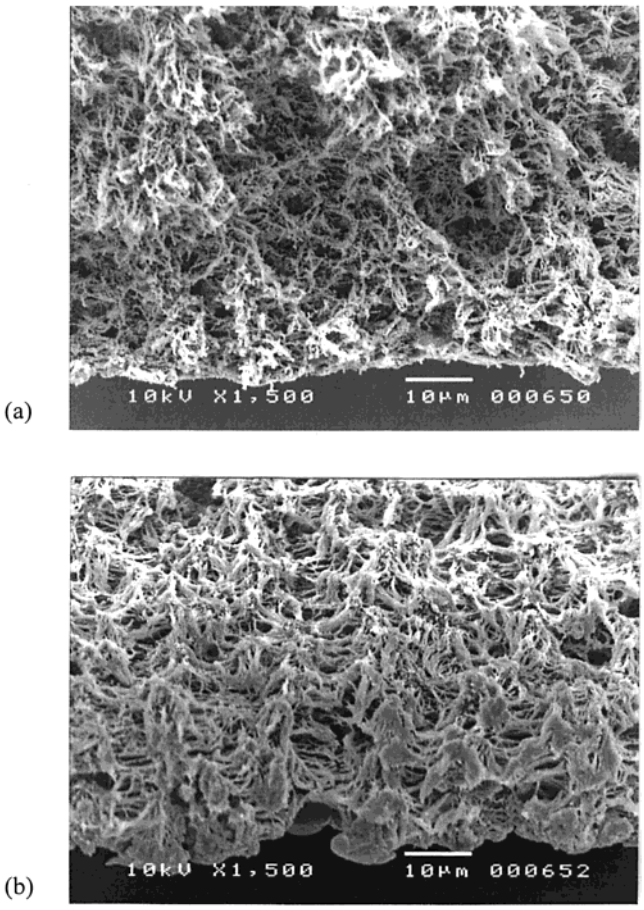

Figure 9. SEM micrograph of the cross section of (a) the untreated ePTFE sheet and (b) the pAAc-grafted ePTFE sheet.

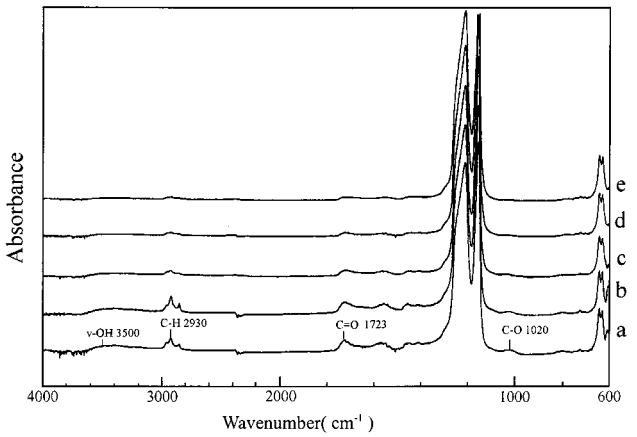

Figure 10. FTIR-ATR microscopy spectra along the cross section of pAAc-grafted ePTFE sheet: (a) 0 μm, (b) 15 μm, (c) 30 μm, (d) 45 μm, and (e) 60 μm beneath the outer surface of the ePTFE sheet.

pAAc-grafted ePTFE was analyzed using FTIR microscopy (as shown in Figure 9). This technique combines visible light microscopy with the ability to collect infrared spectra from microscopic areas and is particularly used for trace analyses.[22] The outer layers were examined separately, revealing different contracting images from the inner part of the sheet, each 15 μm wide. Figure 10 displays the IR spectra of the five outer layers. The main characteristic bands of pAAc at 3500 cm $^{-1}$ (O−H stretching), 2930 cm $^{-1}$ (C−H stretching), 1723 cm $^{-1}$ (C═O stretching), and 1020 cm $^{-1}$ (C−O stretching) are observed for all spectra. The decrease

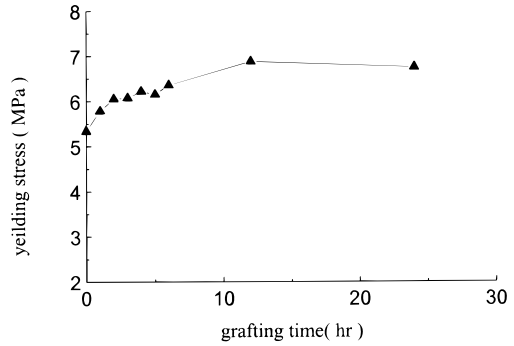

Figure 11. Yielding stress of the pAAc-grafted ePTFE sheet vs grafting time.

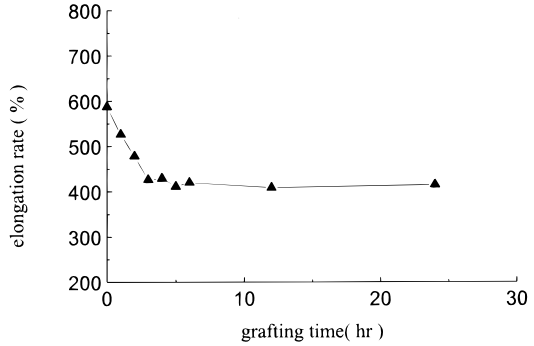

Figure 12. Elongation rate of the pAAc-grafted ePTFE sheet vs grafting time.

of absorbance with increased depth reveals a gradual decrease of pAAc, corresponding to the graft density gradient found in SEM micrographs of the cross section. This finding also confirms that the grafted pAAc is detectable in the ranges of ca. 60 μm beneath the surface of the porous ePTFE sheet.

Mechanical Properties of the ePTFE Sheets. Surface modification to a certain depth may involve the alternation of mechanical properties and its yielding stress and elongation rate vary. Generally, cold plasma treatment onto a material has only a superficial effect (<10 nm) and should not significantly change the bulk strength. This study found only slight variation in the mechanical properties for the ePTFE sheet after the CO_2 plasma treatment. Nevertheless, grafting of pAAc to the ePTFE matrix may influence the bulk properties. Figures 11 and 12 display the variations of the yielding stress and the elongation rate with respect to grafting time for the pAAc-grafted ePTFE sheet. The yielding stress increases by ca. 20%, while the elongation rate decreases by ca. 30%, starting from the grafting time of 3 h. However, further increase of grafting time does not obviously change such mechanical properties. This experimental result indicates that although pAAc grafted only ca. 60 μm to the ePTFE, the mechanical strength of the modified sheet was significantly enhanced.

Conclusion

With CO_2 antenna-coupling plasma treatment, the ePTFE sheet has been effectively activated at surface. The treatment promoted the penetration capability of AAc monomers as well as the graft polymerization of AAc with the ePTFE. The result of FTIR-ATR and XPS measurements suggested that COF species were formed after CO_2 plasma treatment. The plasma-induced ePTFE surfaces exhibited little structural alteration, and

the morphology of the nodes and the stretched fibrils in the ePTFE also remain unchanged. The wettability of the ePTFE surface was increased by the CO_2 plasma treatment and was further increased by subsequent grafting of pAAc. Closely examining SEM micrographs and the corresponding spectra obtained from FTIR microscopy along the cross section of pAAc-grafted ePTFE surface revealed that the depth of the grafted layers beneath the surface is ca. 60 μm. With 60 s of plasma treatment and 3 h grafting time, the yielding stress increased by 20%, and the elongation rate decreased by 30% for the pAAc-grafted ePTFE sheet.

Acknowledgment. The authors thank Chung Yuan Christian University, Taiwan (ROC), for supporting this work.

References and Notes

(1) Karwoski, T.; Matsuzawa, Y. U.S. Pat. 4,718,907, 1988.
(2) Yamada, K.; Ebihara, T.; Gondo, T.; Sakasegawa, K.; Hirata, M. *J. Appl. Polym. Sci.* **1996**, *61*, 1899.
(3) Haque, Y.; Ratner, B. D. *J. Appl. Polym. Sci.* **1986**, *32*, 4369.
(4) Haimovich, B.; Difaz1o, L.; Katz, D.; Zhang, L.; Greco, R. S.; Dror, Y.; Freeman, A. *J. Appl. Polym. Sci.* **1997**, *63*, 1393.
(5) Hegazy, E. A.; Taher, N. H.; Kamel, H. *J. Appl. Polym. Sci.* **1989**, *38*, 1229.
(6) Liao, J. D. *Plasma Chem. Plasma Process.*, in press.
(7) Tan, K. L.; Woon, L. L.; Wong, H. K.; Kang, E. T.; Neoh, K. G. *Macromolecules* **1993**, *26*, 2832.
(8) Kang, E. T.; Tan, K. L.; Kato, K.; Uyama, Y.; Ikada, Y. *Macromolecules* **1996**, *29*, 6872.
(9) Yamada, Y.; Yamada, T.; Tasaka, S.; Inagaki, N. *Macromolecules* **1996**, *29*, 4331.
(10) Liston, E. M. *J. Adhes.* **1989**, *30*, 199.
(11) Coen, M. C.; Groening, P.; Dietler, G.; Schlapbach, L. *J. Appl. Phys.* **1995**, *77*, 5695.
(12) Youxian, D.; Griessert, H. J.; Mau, A. W.-H.; Schmidt, R.; Liesegang, J. *Polymer* **1991**, *32*, 1126.
(13) Costello, A.; McCarthy, T. J. *Macromolecules* **1987**, *20*, 2819.
(14) Badey, J. P.; Espuche, E.; Jugnet, Y.; Sage, D.; Duc, T. M.; Chabert, B. *Polymer* **1994**, *35*, 2472.
(15) Badey, J. P.; Espuchet, E.; Sage, D.; Chabert, B.; Jugnet, Y.; Batier, C.; Duc, T. M. *Polymer* **1996**, *37*, 1377.
(16) Vasilets, V. N.; Hermel, G.; Konig, U.; Werner, C.; Muller, M.; Simon, F.; Grundke, K.; Ikada, Y.; Jacobasch, H. J. *Biomaterial* **1997**, *18*, 1139.
(17) Liao, J. D.; Yu, Y. S.; Wei, P. *Chung Yuan J.* **1999**, *27*−*1*, 1.
(18) Nagarajan, S.; Stachurski, Z. H. *J. Polym. Sci., Phys. Ed.* **1982**, *20*, 989.
(19) Koo, G. *Fluoropolymers*; Wall, L. A., Ed.; John Wiley & Sons: New York, 1972.
(20) Ohta, K.; Iwamoto, R. *Appl. Spectrosc.* **1985**, *39*, 418.
(21) Huang, J.; Chou, W.; Chou, D.; Cheng-Yang, Y. W.; Kau, J. Y. JP 10-237203, 1998.
(22) McEwen, D. J.; Cheever, G. D. *J. Coat. Technol.* **1994**, *65*, 35.

MA990065Q